

Trastuzumab causes antibody-dependent cellular cytotoxicity-mediated growth inhibition of submacroscopic JIMT-1 breast cancer xenografts despite intrinsic drug resistance

Márk Barok,¹ Jorma Isola,⁵ Zsuzsanna Pályi-Krekk,¹ Péter Nagy,¹ István Juhász,² György Vereb,³ Päivikki Kauraniemi,⁵ Anita Kapanen,⁵ Minna Tanner,⁵ György Vereb,¹ and János Szöllösi^{1,4}

Departments of ¹Biophysics and Cell Biology, ²Dermatology, ³Medical Chemistry, ⁴Cell Biology and Signaling Research Group of the Hungarian Academy of Sciences, University of Debrecen, Debrecen, Hungary; and ⁵Institute of Medical Technology, University and University Hospital of Tampere, Tampere, Finland

Abstract

Trastuzumab is a recombinant antibody drug that is widely used for the treatment of breast cancer. Despite encouraging clinical results, some cancers are primarily resistant to trastuzumab, and a majority of those initially responding become resistant during prolonged treatment. The mechanisms of trastuzumab resistance have not been fully understood. We examined the role of antibody-dependent cellular cytotoxicity (ADCC) using JIMT-1 cells that are ErbB2 positive but intrinsically resistant to trastuzumab *in vitro*. Unexpectedly, in experiments mimicking adjuvant therapy of submacroscopic disease *in vivo* (JIMT-1 cells inoculated s.c. in severe combined immunodeficiency mice), trastuzumab was able to inhibit the outgrowth of macroscopically detectable xenograft tumors for up to 5–7 weeks. The effect is likely to be mediated via ADCC because trastuzumab-F(ab')₂ was ineffective in this model. Moreover, *in vitro* ADCC reaction of human leukocytes was equally strong against breast cancer cells intrinsically sensitive (SKBR-3) or resistant (JIMT-1) to trastuzumab or

even against a subline of JIMT-1 that was established from xenograft tumors growing despite trastuzumab treatment. These results suggest that ADCC may be the predominant mechanism of trastuzumab action on submacroscopic tumor spread. Thus, measuring the ADCC activity of patient's leukocytes against the tumor cells may be a relevant predictor of clinical trastuzumab responsiveness *in vivo*. [Mol Cancer Ther 2007;6(7):2065–72]

Introduction

Overexpression of ErbB2 (HER2), a member of the epidermal growth factor (EGF) receptor (EGFR) family of receptor tyrosine kinases, occurs in 20–30% of invasive breast cancers (1–3) and is associated with poor prognosis and rapid relapse (4). Because cancer cell growth is often driven by highly overexpressed oncogenes, even late-stage tumors can be successfully treated with therapies directed against the overexpressed oncoprotein (5, 6). The finding that some of the anti-ErbB2 antibodies can inhibit the growth of cancer cells overexpressing ErbB2 on their surface was a breakthrough in anticancer therapy (7) and led to the development of trastuzumab (Herceptin), a recombinant humanized monoclonal antibody against the extracellular domain of ErbB2. Trastuzumab has a remarkable antitumor effect and is currently used worldwide for the treatment of breast cancer (8, 9). Although the mechanisms underlying the action of trastuzumab are still not fully understood, several molecular effects have been observed. *In vitro* trastuzumab treatment leads to (a) down-regulation of cell surface ErbB2 (10); (b) inactivation of the mitogen-activated protein kinase and phosphoinositide-3-kinase pathways (11, 12); (c) cell cycle arrest in G₁ (13); (d) induction of apoptosis (10); (e) increase in HLA-I-restricted antigen presentation of ErbB2 (14). Furthermore, in *in vivo* models, trastuzumab decreased the microvessel density of breast cancer xenografts (15).

In addition to the direct effects on cancer cells, several lines of evidence suggested that antibody-dependent cellular cytotoxicity (ADCC) plays an important role in the antitumor activity of trastuzumab. Clynes et al. showed that the activity of trastuzumab on breast cancer xenografts was attenuated in knock-out mice lacking activating FcγRIII receptors. Furthermore, the administration of trastuzumab lacking functional FcR binding capability resulted in similarly attenuated response in wild-type mice (16). In addition, Spiridon et al. found that trastuzumab-F(ab')₂ and a mixture of F(ab')₂ fragments of three anti-ErbB2

Received 12/11/06; revised 4/10/07; accepted 5/25/07.

Grant support: Hungarian Academy of Sciences grants OTKA T043061 and F049025, European Commission grants LSHB-CT-2004-503467 and LSHC-CT-2005-018914, Finnish Cancer Foundation, Sigrid Juselius Foundation, and Tampere University Hospital Research Foundation.

The costs of publication of this article were defrayed in part by the payment of page charges. This article must therefore be hereby marked *advertisement* in accordance with 18 U.S.C. Section 1734 solely to indicate this fact.

Note: M. Barok and J. Isola contributed equally to the work.

Requests for reprints: János Szöllösi, Medical and Health Science Center, Department of Biophysics and Cell Biology, University of Debrecen, 1 Egyetem sqr., Debrecen 4010, Hungary. Phone: 36-52412623; Fax: 36-52532201. E-mail: szollo@dote.hu

Copyright © 2007 American Association for Cancer Research.

doi:10.1158/1535-7163.MCT-06-0766

immunoglobulin G (IgG) exerted significantly reduced responses compared with those of trastuzumab IgG and the mixture of the three anti-ErbB2 IgGs in mice xenografted with trastuzumab-sensitive breast cancer cells (17).

Despite encouraging clinical results, some cancers are primarily resistant to trastuzumab, and a majority of those initially responding become resistant during prolonged treatment (8, 18). The mechanisms of trastuzumab resistance have not been fully elucidated. The following mechanisms have been implicated: (a) autocrine production of EGF-related ligands (19); (b) activation of the insulin-like growth factor-I (IGF-I) receptor pathway (20); (c) masking of the trastuzumab epitope by MUC4, a cell surface sialomucin (21, 22); (d) loss of PTEN function (23); (e) impaired ADCC reaction (24, 25).

Possible mechanisms of trastuzumab resistance have been studied in detail using the breast cancer cell line JIMT-1 established from the pleural metastasis of a patient who was clinically resistant to trastuzumab. JIMT-1 cells are resistant to trastuzumab *in vitro* and also *in vivo*, if therapy is initiated 45 days after establishing xenografts (26). In the current paper, we show that in spite of trastuzumab resistance of JIMT-1 cells *in vitro* and their macroscopic tumors *in vivo*, proliferation of these cells inoculated s.c. into severe combined immunodeficiency (SCID) mice is effectively inhibited for up to 5–7 weeks if trastuzumab treatment is started immediately. Because trastuzumab-F(ab')₂ exerts no similar effect, the mechanism of early-stage trastuzumab sensitivity is likely based on ADCC. We found no difference in the *in vitro* ADCC activity of human leukocytes against JIMT-1 or SKBR-3 breast cancer cells, although the latter are intrinsically trastuzumab-sensitive *in vitro*, suggesting that the compromised immune response of the host or *in vivo* masking of the tumor cell surface may play key roles in the development of the trastuzumab nonresponsive phenotype.

Materials and Methods

Cells

JIMT-1, the ErbB2-positive human breast cancer cell line was grown in Ham's F-12/DMEM (1:1) supplemented with 10% FCS, 60 units/L insulin, and antibiotics (26). SKBR-3 and BT-474 cell lines were obtained from the American Type Culture Collection and cultured according to specifications.

Xenograft Tumors

The SCID C.B-17 *scid/scid* (originated from the laboratory of Fox Chase Cancer Center, Philadelphia, PA) and *nu/nu* nude mouse population (Harlan Netherland, Horst, the Netherlands) were housed in a pathogen-free environment. Only nonleaky SCID mice with murine IgG levels below 100 ng/mL were used in this study (27). Seven-week-old female nude or SCID mice were given a single s.c. injection of 5×10^6 JIMT-1 cells suspended in 150 μ L Hanks' A buffer and mixed with an equal volume of Matrigel (BD Matrigel, BD Biosciences). Tumor volumes were derived as the product of the length, width, and height of the tumor measured once a week with a caliper.

Trastuzumab and trastuzumab-F(ab')₂ were given at a dose of 5 and 25 μ g/g, respectively, by weekly i.p. injection. The five times greater amount of administered F(ab')₂ was chosen based on the different half-lives of IgG and F(ab')₂ *in vivo* (17). Control mice were treated with weekly i.p. injection of 100 μ L physiologic saline (saline) or rituximab (a humanized anti-CD20 antibody) at a dose of 5 μ g/g. Animals were euthanized by CO₂ inhalation. The experiments were done with the approval of the Ethical Committee of the University of Debrecen.

Establishment of Sublines from JIMT-1 Xenografts

The JIMT-1 X⁻ and the JIMT-1 X⁺ cell lines were derived from the tumor of mice treated continuously with saline and trastuzumab, respectively. Animals were euthanized, and the tumors were removed and cut into small pieces with a sterile blade, washed twice with sterile PBS, and placed in culture dishes in medium containing F-12/DMEM (1:1) supplemented with 20% FCS, 60 units/L insulin, and antibiotics. The medium of JIMT-1 X⁺ cells also contained 10 μ g/mL trastuzumab (28). After 3 days, debris and dead cells were removed, and the medium was refreshed. Confluent cultures were trypsinized and split at a ratio of 1:2, using the same medium but with only 10% FCS. JIMT-1 X⁺ cells have been grown in the presence of 10 μ g/mL trastuzumab ever since the establishment of the cell line.

Antibodies

Herceptin (trastuzumab) and Mabthera (rituximab) were purchased from Roche Ltd. Monoclonal antibody (mAb) against ErbB2 (erbB2-76.5 IgG₁) was produced from the supernatant of the erbB2-76.5 hybridoma (kindly provided by Y. Yarden, Weizmann Institute of Science, Rehovot, Israel) and purified using protein A affinity chromatography.

Conjugation of Antibodies with Fluorescent Dyes

Covalent binding of AlexaFluor 546 (Molecular Probes) to the erbB2-76.5 antibody was carried out according to the manufacturer's instructions. The dye/protein labeling ratio was ~3:1.

Preparation and Testing of Trastuzumab-F(ab')₂ Fragment

Trastuzumab IgG (20 mg) was dissolved in 20 mmol/L acetate buffer (pH, 4.5) and dialyzed thrice into the same buffer and concentrated using Centricon-10 tubes (Millipore Corp.). Digestion was done by adding 0.5 mL immobilized pepsin (Pierce Biotechnology) at 37°C for 6 h. The reaction was stopped by 10 mL 2 mol/L Tris-HCl (pH, 8.2), and digested trastuzumab was filtered through a 0.22- μ m Millex filter (Millipore Corp.) to remove immobilized pepsin bound to agarose beads and concentrated to 1 mL using Centricon-50 tubes (Millipore Corp.). Trastuzumab-F(ab')₂ fragments and undigested trastuzumab were separated by high-performance liquid chromatography using a column (10 \times 800 mm) filled with Sephacryl S-300 (Pharmacia LKB) and an eluant of 50 mmol/L sodium phosphate (pH, 7.0). Fractions of 0.5 mL were collected and tested using nonreducing SDS-PAGE analysis. Fractions containing trastuzumab-F(ab')₂ without contamination of undigested trastuzumab were merged,

concentrated, and stored at -20°C . The quality of trastuzumab-F(ab')₂ was tested on SKBR-3 cells; trastuzumab-F(ab')₂ bound to the cells competed with intact trastuzumab and bound no Fc-specific secondary antibodies (data not shown).

In vitro Assay of Drug Sensitivity

The effects of trastuzumab and trastuzumab-F(ab')₂ on the growth of JIMT-1, SKBR-3, and BT-474 cells were evaluated using the AlamarBlue method (TREK Diagnostic Systems, Inc.). Exponentially growing cells were harvested and plated in single wells of a 96-well flat-bottomed tissue culture plate at defined densities, ranging from 4,500–8,000 cells per well depending on the cell line. After overnight culture, the regular medium was exchanged to medium containing 0, 1, 10, or 100 $\mu\text{g}/\text{mL}$ trastuzumab or trastuzumab-F(ab')₂. Cell viability was tested after 72 h of treatment according to the manufacturer's instructions. Fluorescence was detected at an excitation of 544 nm, and emission was detected at 590 nm using a Wallac Victor2 plate reader (Perkin-Elmer).

Immunohistochemistry

S.c. tumors were removed from anesthetized mice, covered with Shandon Cryomatrix (Thermo Electron Corporation, Anatomical Pathology USA Clinical Diagnostics), and stored in liquid nitrogen. Cryosections, 20 μm thick, were cut using a SHANDON AS-620E Cryotome (Thermo Electron Corporation) on silanized slides. Samples were fixed in 4% formaldehyde for 30 min and were washed twice in PBS with 1% bovine serum albumin (BSA; pH, 7.4) for 20 min at room temperature. Slides were labeled with a saturating concentration (10–20 $\mu\text{g}/\text{mL}$) of dye-conjugated antibody in 100 μL PBS containing 1% BSA overnight on ice, washed twice with PBS, and covered with 15 μL Mowiol (Merck) to avoid bleaching of the fluorescent dyes.

Confocal Microscopy

A Zeiss LSM 510 confocal laser-scanning microscope (Carl Zeiss AG) was used to image samples. AlexaFluor 546 was excited with the 543-nm line of a green He-Ne laser, and emission measured between 560 and 615 nm. Fluorescence images were taken as 1- μm optical sections using a 63 \times (numerical aperture = 1.4) oil immersion objective.

Image Analysis

Confocal microscopic images were analyzed with the DipImage toolbox (Delft University of Technology, Delft, the Netherlands) under Matlab (Mathworks Inc., Natick, MA). The cell membrane was identified by a manually seeded watershed algorithm (29) using a custom-written interactive algorithm implemented in DipImage/Matlab. The cell membrane was used as a mask, and the fluorescence intensity was evaluated only in pixels under the mask.

In vitro ADCC Assay

ADCC assays were done as described previously (17, 30) with modifications. Peripheral blood mononuclear cells (PBMC) were separated from the blood of healthy donors by Ficoll density gradient centrifugation (Histopaque-1077, Sigma-Aldrich). The fraction containing PBMCs was

resuspended in DMEM containing 10% FCS. JIMT-1, JIMT X⁻, JIMT X⁺, and SKBR-3 tumor cells were harvested, washed once in PBS containing 1% bovine serum albumin (BSA), and labeled with 5- (and 6)-carboxyfluorescein

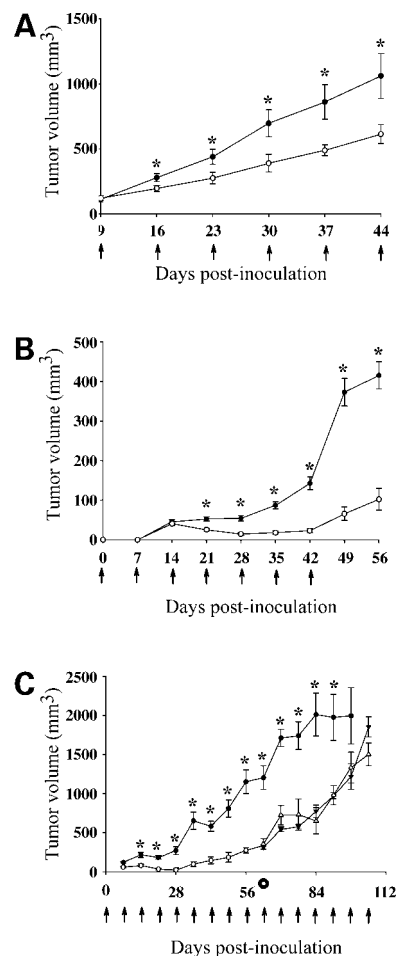


Figure 1. **A**, trastuzumab partially inhibits growth of established early-stage JIMT-1 xenograft tumors in SCID mice. About 5×10^6 JIMT-1 cells were injected s.c. into SCID mice, and weekly treatment (arrows) with trastuzumab (\circ) or saline (\bullet) was initiated 9 d after tumor inoculation, when the tumors were palpable ($n = 8$ in both groups). Tumor growth was significantly reduced in the trastuzumab-treated group versus the control group between days 16 and 44. *, $P < 0.05$. **B**, trastuzumab inhibits outgrowth of JIMT-1 tumors in nude mice. Trastuzumab (\circ , $n = 7$) or rituximab (\bullet , $n = 7$) treatment of nude mice injected with 5×10^6 tumor cells was started on the day of tumor cell inoculation and continued on a weekly basis (arrows). Trastuzumab therapy was suspended on day 42. Tumor growth was significantly reduced in the trastuzumab-treated group versus the control group between days 21 and 56. *, $P < 0.05$. **C**, trastuzumab markedly hinders early tumor outgrowth from JIMT-1 cells inoculated in SCID mice. Trastuzumab (\circ , $n = 8$) or saline (\bullet , $n = 8$) treatment (arrows) of mice injected with 5×10^6 tumor cells was started on the day of tumor cell inoculation and continued on a weekly basis. In four out of the eight trastuzumab-treated mice, trastuzumab administration was suspended (\blacktriangledown) on week 9 (marked by \bullet), whereas it was continued for another 6 wks in the other four (\triangle). Tumor growth was significantly reduced in the trastuzumab-treated group versus the control group between days 14 and 91. *, $P < 0.05$. There was no significant difference between the "suspended trastuzumab" and "continued trastuzumab" subgroups. Note that tumor volumes are plotted on different scales.

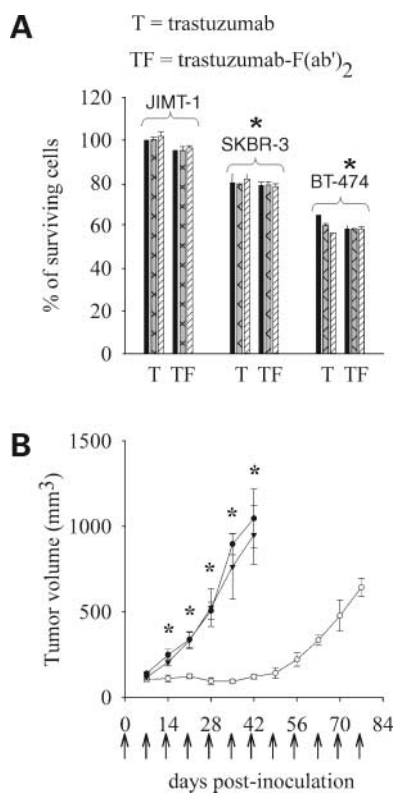


Figure 2. *In vitro* and *in vivo* effects of trastuzumab-F(ab')₂. **A**, trastuzumab-F(ab')₂ acts *in vitro* similar to whole trastuzumab. Trastuzumab-F(ab')₂ inhibited the growth of trastuzumab-sensitive cell lines SKBR-3 and BT-474 *in vitro* as effectively as trastuzumab IgG. JIMT-1 cells were resistant *in vitro* to both trastuzumab-IgG and trastuzumab-F(ab')₂. T, trastuzumab; TF, trastuzumab-F(ab')₂. Doses: black column, 1 μg/mL; cross-hatched column, 10 μg/mL; hatched column, 100 μg/mL. Neither trastuzumab whole IgG nor trastuzumab-F(ab')₂ fragment had any inhibitory effect on JIMT-1 cells *in vitro*, whereas both had significant inhibitory effect on SKBR-3 and BT-474 cells as compared with their effect on JIMT-1 cells. *, $P < 0.05$. **B**, lack of effect of trastuzumab-F(ab')₂ on JIMT-1 xenografts. SCID mice injected s.c. with 5×10^6 JIMT-1 cells were treated i.p. on a weekly basis (arrows) with saline (●, $n = 8$), trastuzumab IgG (○, $n = 8$), or trastuzumab-F(ab')₂ (▼, $n = 8$), starting on the day of inoculation. Tumor growth was significantly reduced in the trastuzumab-treated group versus the saline-treated group between days 14 and 42. *, $P < 0.05$. There was no significant difference between the trastuzumab-F(ab')₂ and the saline-treated groups.

diacetate, succinimidyl ester (CFDA, SE; Molecular Probes, Inc.) at a concentration of 10 μmol/L at 37°C for 10 min. Then, tumor cells were washed thrice with DMEM containing 10% FCS and 1% BSA to remove unreacted and unbound CFDA, SE. Between the washing steps, cells were incubated in the same medium at 37°C for 5 min. Finally, the labeled target cells were resuspended in DMEM containing 10% FCS and mixed with PBMCs at effector/target ratios (E/T) of 2:1, 6:1, 15:1, 30:1, and 60:1. Trastuzumab, rituximab, or trastuzumab-F(ab')₂ were added to the mixed suspensions at a concentration 100 μg/mL. The samples were incubated at 37°C for 8 h followed by staining of dead cells with 50 μg/mL

propidium iodide. Cells were analyzed on a Becton Dickinson FACScan flow cytometer (Mountain View). The negative control sample was prepared identically, but did not contain PBMCs. Tumor cells killed by 4% formaldehyde served as the positive control. The percentage of cells killed was calculated according the following formula: (% of living cells in the negative control – % of living cells in the sample) / % of living cells in the negative control.

Statistical Analysis

Data are expressed as the mean ± SE. The statistical significance of the differences between means were determined using Student's *t* test for two samples after verifying that data passed the normality test and the groups compared have equal variance. Differences were statistically significant at $P < 0.05$.

Results

Effect of Trastuzumab on Established JIMT-1 Xenograft Tumors

We have shown previously that established JIMT-1 xenograft tumors (tumor volume 200–500 mm³) are insensitive to trastuzumab treatment in immunodeficient *nu/nmri* mice (26). First, we tested the effects of trastuzumab on smaller xenograft tumors of 100–200 mm³ volume in SCID mice that had been inoculated s.c. with 5×10^6 JIMT-1 cells in suspension only 9 days before treatment. Weekly treatment with trastuzumab or saline was continued until the end of the experiment. Tumor growth was partially but significantly inhibited by trastuzumab from days 16 to 44 ($P < 0.05$) when compared with the control group (Fig. 1A).

Effect of Trastuzumab on Nonestablished JIMT-1 Tumors in Nude or SCID Mice

Because the growth of small JIMT-1 xenograft tumors was partially inhibited by trastuzumab, we next studied the effect of trastuzumab treatment started at the time when 5×10^6 JIMT-1 cells were inoculated s.c. into nude or SCID mice.

Tumors were formed in all of the seven nude mice treated with rituximab (a negative control antibody directed to CD20, a transmembrane protein not expressed by JIMT-1 cells; data not shown), whereas palpable tumors developed only in two of seven trastuzumab-treated animals. Trastuzumab administration was suspended on day 42 when the inhibitory effect of trastuzumab was obvious as compared with rituximab treatment. Trastuzumab had a significant inhibitory effect on tumor growth from days 21 to 56 ($P < 0.05$). After stopping trastuzumab administration, tumors started to grow in the two nude mice whose tumors were palpable earlier (Fig. 1B).

The growth of tumors in all trastuzumab-treated SCID mice was minimal for up day 42. From the fifth week onward, the tumors started to grow exponentially in all (8/8) trastuzumab-treated mice. At this time point, trastuzumab treatment was suspended in half of the treated animals and continued for another 6 weeks in the rest of the animals. There was no difference in the rate of

tumor growth between these two subgroups, indicating complete resistance to trastuzumab (Fig. 1C). The effect of trastuzumab on tumor growth was significant from days 14 to 91 ($P < 0.05$).

Treatment of JIMT-1 Tumors with Trastuzumab-F(ab')₂

Because JIMT-1 cells are intrinsically resistant to trastuzumab, we hypothesized that the effects on submacro-

scopic xenografts are owed to ADCC reaction. We have therefore generated trastuzumab-F(ab')₂, which binds ErbB2 with high affinity and exhibits *in vitro* growth inhibition equivalent to that of intact trastuzumab IgG in both SKBR-3 and BT-474 cell cultures (Fig. 2A). When using this trastuzumab-F(ab')₂ for weekly treatment of SCID mice inoculated with 5×10^6 JIMT-1 cells, on a weekly basis, no effect on xenograft tumor growth was seen as compared with saline treatment. In the parallel positive control, intact trastuzumab IgG significantly inhibited the growth of JIMT-1 tumors (from days 14 to 42; $P < 0.05$) similarly to findings in the previous experiment (Fig. 2B).

Cell Surface Expression Level of ErbB2 in JIMT-1 Xenografts

To investigate whether trastuzumab IgG and trastuzumab-F(ab')₂ were able to down-regulate ErbB2 *in vivo*, fast frozen tissue sections were labeled with a fluorescent anti-ErbB2 antibody erbB2-76.5. The ErbB2 expression level of trastuzumab-treated tumors was ~50% lower than that of saline-treated cells. Quantitative image analysis revealed that trastuzumab-F(ab')₂ and trastuzumab IgG were equally effective in down-regulating ErbB2 expression. Six weeks after suspension of trastuzumab treatment, the ErbB2 expression level returned to almost as high as in control mice (Fig. 3A and B).

In vitro ADCC Activity against Trastuzumab-Sensitive and Trastuzumab-Resistant Breast Cancer Cell Lines

The fact that trastuzumab-F(ab')₂, unlike trastuzumab IgG, was ineffective against JIMT-1 xenografts *in vivo* suggested that the immune effector cells of SCID mice are responsible for growth retardation, irrespective of intrinsic cellular resistance. We next did *in vitro* ADCC assays using human peripheral leukocytes (PBMCs) as effector cells. The baseline killing of tumor target cells by PBMCs in the presence of rituximab (IgG control) was low; there was no significant difference in target cell killing between assays done with rituximab or with trastuzumab-F(ab')₂. In contrast, the presence of trastuzumab IgG significantly increased killing of all breast cancer cell lines ($P < 0.05$). The ADCC activity of PBMCs evoked by trastuzumab was equally strong against trastuzumab-sensitive (SKBR-3) or trastuzumab-resistant (JIMT-1) breast cancer cells, with dose-dependent cell death reaching ~50–60% killing at an effector/target ratio of 60:1. In addition to the native JIMT-1 cells, two sublines, JIMT-1 X⁻, recovered from xenografted mice treated with saline, and JIMT-1 X⁺, a superresistant subline recovered after continuous treatment with trastuzumab, were as sensitive to ADCC as SKBR-3 (Fig. 4).

Discussion

It is well documented that trastuzumab acts directly in cancer cell signaling, as well as indirectly via the immune system. We studied the *in vivo* effects of trastuzumab using JIMT-1 cells that are intrinsically resistant to trastuzumab *in vitro*, despite ErbB2 gene amplification and receptor

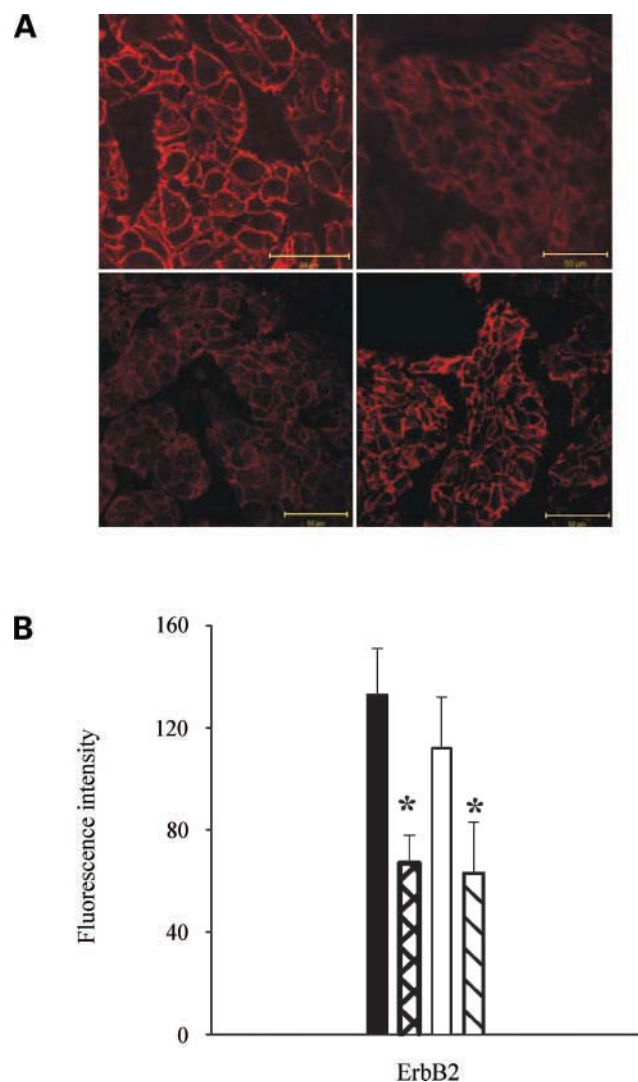


Figure 3. Changes in ErbB2 level after trastuzumab IgG and trastuzumab-F(ab')₂ treatment. **A**, immunofluorescent images of frozen sections prepared from JIMT-1 xenografts. Mice were treated with saline (*top left*), trastuzumab-F(ab')₂ (*top right*), trastuzumab IgG continuously (*bottom left*), or trastuzumab IgG suspended 6 weeks before sacrificing the animal (*bottom right*). ErbB2 was labeled with AlexaFluor 543-conjugated erbB2-76.5 antibodies. Images were taken with identical microscope settings. **B**, quantitative analysis of membrane fluorescence. Five images from each type of treatment were analyzed as described in Materials and Methods, and the average fluorescence intensity registered in membranes was plotted. *Black column*, saline; *cross-hatched column*, continuous trastuzumab IgG; *empty column*, suspended trastuzumab IgG; *hatched column*, continuous trastuzumab-F(ab')₂. Continuous trastuzumab IgG and trastuzumab-F(ab')₂ treatment decreased ErbB2 levels significantly. *, $P < 0.05$.

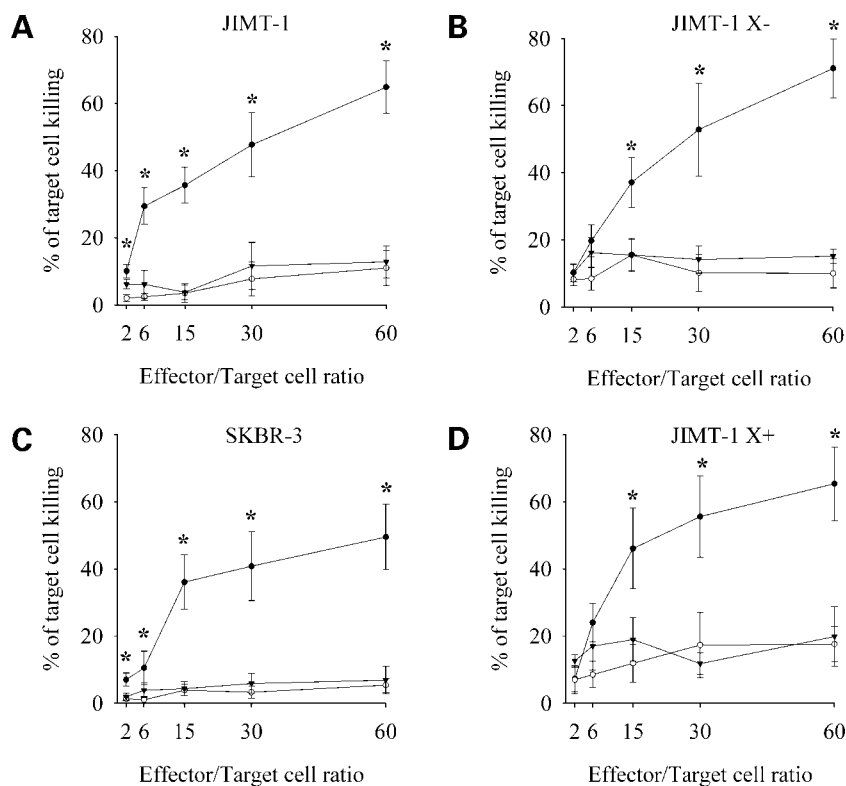


Figure 4. *In vitro* trastuzumab-mediated ADCC against ErbB2-positive tumor cells. Target tumor cells [(A) JIMT-1; (B) JIMT-1 X-; (C) SKBR-3; (D) JIMT-1 X+] were labeled with CFDA, SE, then mixed with PBMCs freshly isolated from peripheral blood at effector/target ratios of 2:1, 6:1, 15:1, 30:1, and 60:1. Trastuzumab (●), trastuzumab-F(ab')₂ (▼), or rituximab (○) were added to the mixed samples at a concentration of 100 μg/mL. After an 8-h incubation at 37°C, samples were stained with propidium iodide and analyzed by flow cytometry. The percentage of killed cells was calculated as described in Materials and Methods. In all cell lines, tumor cell killing was significantly higher in the presence of trastuzumab whole IgG than that observed in the presence of trastuzumab-F(ab')₂ fragment when the effector/target cell ratio was 15 or above. *, $P < 0.05$. No significant difference was observed between the effects of rituximab and trastuzumab-F(ab')₂. Similarly, no significant differences were observed among the cell lines in the killing effect of trastuzumab-mediated ADCC.

overexpression. The JIMT-1 cell line is a unique patient-derived model system, which allows for separately studying the direct and immune-mediated growth-inhibitory mechanisms of trastuzumab when using *in vitro* and xenograft models (26).

Our main and unexpected finding was that trastuzumab caused a significant growth inhibition of the outgrowth of macroscopic JIMT-1 xenograft tumors in both nude and SCID mice. The effect was probably mediated via the Fc portion of trastuzumab IgG because the F(ab')₂ fragment of trastuzumab was ineffective in the SCID mouse model system, in spite of inhibiting proliferation of trastuzumab-sensitive cells *in vitro* equally well as intact trastuzumab IgG. We attribute the Fc-mediated effects of trastuzumab to ADCC because both nude and SCID mice have functioning macrophages and natural killer cells (31–33) capable of killing tumor cells by ADCC. The antitumor effect of trastuzumab was stronger in nude mice because it prevented the formation of palpable tumors in five out of seven nude mice, whereas it only slowed the growth rate of JIMT-1 xenografts in SCID mice. This phenomenon can be explained by the more severe immunodeficiency of SCID mice lacking both T and B cells (31) compared with nude mice capable of mounting a B cell response against thymus-independent antigens (34, 35). These findings reflect the central role of the immune system in mediating the effects of trastuzumab *in vivo*. In a previous study, Clynes et al. inoculated trastuzumab-sensitive BT-474 cells into knock-

out mice lacking activating FcγIII receptors. In this model system, the antitumor activity of trastuzumab was reduced but not ablated: about 25% of the effect was retained (16). In the same manner, treatment of wild-type mice with the mutated form of 4D5, the parent antibody of trastuzumab, which was made unable to bind to Fc receptors, had a similar partial effect (16). These results indicate that in the case of BT-474 cells, trastuzumab probably triggers both the intrinsic growth-inhibitory and apoptotic regulatory pathways, as well as evokes ADCC. In the case of the intrinsically resistant JIMT-1 cells, the mechanism of action of trastuzumab seems to be exclusively ADCC.

The mutual independence of the intrinsic and immune-mediated effects was further evidenced by *in vitro* ADCC experiments using human peripheral leukocytes as effector cells. The capacity of these cells to kill JIMT-1 and SKBR-3 cells in the presence of trastuzumab by ADCC was the same despite significant differences in the direct drug-sensitivity assays. Moreover, we found that the downmodulation of ErbB2 receptor from the cell surface upon trastuzumab treatment, which has previously been postulated as the central phenomenon for direct growth inhibition, (10, 36) seems to be mechanistically unrelated to the action of trastuzumab *in vivo*.

The other main finding in our study was that the capacity of the ADCC reaction to inhibit growth of xenograft tumors was clearly dependent on tumor cell load and possibly also the accessibility of tumor cells to effectors. Whereas s.c.

inoculated JIMT-1 cells were initially sensitive to trastuzumab, this sensitivity was gradually lost as the tumors grew larger in size. These results contrast those published for intrinsically trastuzumab-sensitive BT-474 xenografts, where trastuzumab treatment is highly effective also in the case of larger established tumors (17, 37).

Theoretically, it is possible that JIMT-1 xenografts had acquired new resistance mechanisms against ADCC during trastuzumab treatment. However, we find this unlikely because the subline JIMT-X+, generated from a trastuzumab-treated JIMT-1 xenograft, did not differ from the parental JIMT-1 cells in the *in vitro* ADCC assays. JIMT-1 X+ cells were able to form xenografts in SCID mice, and the growth of the xenografts was reduced by trastuzumab administration, suggesting that JIMT-1 X+ cells were initially sensitive to trastuzumab also *in vivo*, although trastuzumab resistance has developed after 3 weeks (data not shown). Thus, it is more likely that in SCID mice, the capacity for ADCC is gradually exhausted with increasing tumor load. These results are coherent with recent clinical observations indicating a surprisingly high efficacy of adjuvant trastuzumab therapy applied at early stages of the tumor, compared with less striking results achieved in overtly metastatic disease (38–40). If the clinical effects of trastuzumab on submacroscopic disease are mainly derived from ADCC, which, based on the present observations, seems to lose its efficacy as the tumor grows, it is possible that clinical benefits may decrease during extended follow-up.

Finally, our results may have important implications in the search for putative trastuzumab resistance mechanisms. Many groups, including ours, have characterized breast cancer cell lines and clinical tumor specimens for intrinsic cellular features such as ErbB2 protein turnover, autocrine production of EGF-related ligands (19), activation of the IGF-I receptor pathway (20), loss of PTEN function (23), steric hindrance of ErbB2 on the cell surface (22, 41). Although these intrinsic mechanisms may partly underlie nonresponsiveness to trastuzumab, our results clearly stress the importance of immune-mediated mechanisms, the capacity of which may vary depending on tumor volume, either as a function of gross cell numbers, or of accessibility of tumor cells by effector cells. In the clinical setting, the importance of immune mechanisms has been highlighted by Gennari et al. (42), who have showed that the only statistically significant difference between trastuzumab-responding and nonresponding patients was in the ADCC activity of peripheral blood leukocytes. Unfortunately, currently available ADCC assays are technically too complicated for routine clinical diagnostics. Thus, the development of simpler ADCC assays or new surrogate markers (such as FcγRIIIa gene polymorphisms; ref. 43) may be of significant help in optimal patient selection for trastuzumab therapy. In the future, new approaches such as anti-ErbB2 antibodies engineered for higher affinity Fc receptor binding may also lead to improved therapeutic efficacy of ErbB2-positive breast cancers (44).

Acknowledgments

We acknowledge the excellent technical assistance of Ferenc Bostyán and Géza Mók in performing animal studies.

References

- Ross JS, Fletcher JA, Linette GP, et al. The Her-2/neu gene and protein in breast cancer 2003: biomarker and target of therapy. *Oncologist* 2003; 8:307–25.
- Slamon DJ, Godolphin W, Jones LA, et al. Studies of the HER-2/neu proto-oncogene in human breast and ovarian cancer. *Science* 1989;244: 707–12.
- Slamon DJ, Clark GM, Wong SG, Levin WJ, Ullrich A, McGuire WL. Human breast cancer: correlation of relapse and survival with amplification of the HER-2/neu oncogene. *Science* 1987;235:177–82.
- Paik S, Liu ET. HER2 as a predictor of therapeutic response in breast cancer. *Breast Dis* 2000;11:91–102.
- Gorre ME, Mohammed M, Ellwood K, et al. Clinical resistance to STI-571 cancer therapy caused by BCR-ABL gene mutation or amplification. *Science* 2001;293:876–80.
- Weinstein IB. Cancer. Addiction to oncogenes—the Achilles heel of cancer. *Science* 2002;297:63–4.
- Hudziak RM, Lewis GD, Winget M, Fendly BM, Shepard HM, Ullrich A. p185HER2 monoclonal antibody has antiproliferative effects *in vitro* and sensitizes human breast tumor cells to tumor necrosis factor. *Mol Cell Biol* 1989;9:1165–72.
- Slamon DJ, Leyland-Jones B, Shak S, et al. Use of chemotherapy plus a monoclonal antibody against HER2 for metastatic breast cancer that overexpresses HER2. *N Engl J Med* 2001;344:783–92.
- Baselga J. Clinical trials of Herceptin(R) (trastuzumab). *Eur J Cancer* 2001;37 Suppl 1:18–24.
- Cuello M, Ettenberg SA, Clark AS, et al. Down-regulation of the erbB-2 receptor by trastuzumab (Herceptin) enhances tumor necrosis factor-related apoptosis-inducing ligand-mediated apoptosis in breast and ovarian cancer cell lines that overexpress erbB-2. *Cancer Res* 2001;61: 4892–900.
- Nagy P, Jenei A, Damjanovich S, Jovin TM, Szöllösi J. Complexity of signal transduction mediated by ErbB2: clues to the potential of receptor-targeted cancer therapy. *Pathol Oncol Res* 1999;5:255–71.
- Slivkowsky MX, Lofgren JA, Lewis GD, Hotaling TE, Fendly BM, Fox JA. Nonclinical studies addressing the mechanism of action of trastuzumab (Herceptin). *Semin Oncol* 1999;26:60–70.
- Lane HA, Motoyama AB, Beuvink I, Hynes NE. Modulation of p27/Cdk2 complex formation through 4D5-mediated inhibition of HER2 receptor signaling. *Ann Oncol* 2001;12 Suppl 1:S21–22.
- Kono K, Sato E, Naganuma H, et al. Trastuzumab (Herceptin) enhances class I-restricted antigen presentation recognized by HER-2/neu-specific T cytotoxic lymphocytes. *Clin Cancer Res* 2004;10: 2538–44.
- Izumi Y, Xu L, di Tomaso E, Fukumura D, Jain RK. Tumour biology: Herceptin acts as an anti-angiogenic cocktail. *Nature* 2002;416:279–80.
- Clynes RA, Towers TL, Presta LG, Ravetch JV. Inhibitory Fc receptors modulate *in vivo* cytotoxicity against tumor targets. *Nat Med* 2000;6:443–6.
- Spiridon CI, Guinn S, Vitetta ES. A comparison of the *in vitro* and *in vivo* activities of IgG and F(ab')₂ fragments of a mixture of three monoclonal anti-Her-2 antibodies. *Clin Cancer Res* 2004;10:3542–51.
- Esteva FJ, Valero V, Booser D, et al. Phase II study of weekly docetaxel and trastuzumab for patients with HER-2-overexpressing metastatic breast cancer. *J Clin Oncol* 2002;20:1800–8.
- Motoyama AB, Hynes NE, Lane HA. The efficacy of ErbB receptor-targeted anticancer therapeutics is influenced by the availability of epidermal growth factor-related peptides. *Cancer Res* 2002;62:3151–8.
- Lu Y, Zi X, Pollak M. Molecular mechanisms underlying IGF-I-induced attenuation of the growth-inhibitory activity of trastuzumab (Herceptin) on SKBR3 breast cancer cells. *Int J Cancer* 2004;108:334–41.
- Price-Schiavi SA, Jepsen S, Li P, et al. Rat Muc4 (sialomucin complex) reduces binding of anti-ErbB2 antibodies to tumor cell surfaces, a potential mechanism for Herceptin resistance. *Int J Cancer* 2002;99: 783–91.
- Nagy P, Friedländer E, Tanner M, et al. Decreased accessibility and

- lack of activation of ErbB2 in JIMT-1, a Herceptin-resistant, MUC4-expressing breast cancer cell line. *Cancer Res* 2005;65:473–82.
23. Nagata Y, Lan KH, Zhou X, et al. PTEN activation contributes to tumor inhibition by trastuzumab, and loss of PTEN predicts trastuzumab resistance in patients. *Cancer Cell* 2004;6:117–27.
24. Kono K, Takahashi A, Ichihara F, Sugai H, Fujii H, Matsumoto Y. Impaired antibody-dependent cellular cytotoxicity mediated by Herceptin in patients with gastric cancer. *Cancer Res* 2002;62:5813–7.
25. Mimura K, Kono K, Hanawa M, et al. Trastuzumab-mediated antibody-dependent cellular cytotoxicity against esophageal squamous cell carcinoma. *Clin Cancer Res* 2005;11:4898–904.
26. Tanner M, Kapanen AI, Junntila T, et al. Characterization of a novel cell line established from a patient with Herceptin-resistant breast cancer. *Mol Cancer Ther* 2004;3:1585–92.
27. Bosma GC, Fried M, Custer RP, Carroll A, Gibson DM, Bosma MJ. Evidence of functional lymphocytes in some (leaky) scid mice. *J Exp Med* 1988;167:1016–33.
28. Kute T, Lack CM, Willingham M, et al. Development of Herceptin resistance in breast cancer cells. *Cytometry A* 2004;57:86–93.
29. Gonzalez RC, Woods RE, Eddins SL. Segmentation using the watershed transform. In: *Digital image processing using Matlab*. Upper Saddle River, NJ: Pearson Prentice Hall: 2004; p. 417–425.
30. Flieger D, Gruber R, Schlimok G, Reiter C, Pantel K, Riethmuller G. A novel non-radioactive cellular cytotoxicity test based on the differential assessment of living and killed target and effector cells. *J Immunol Methods* 1995;180:1–13.
31. Bosma MJ, Carroll AM. The SCID mouse mutant: definition, characterization, and potential uses. *Annu Rev Immunol* 1991;9:323–50.
32. Cheers C, Waller R. Activated macrophages in congenitally athymic “nude mice” and in lethally irradiate mice. *J Immunol* 1975;115:844–7.
33. Hasui M, Saikawa Y, Miura M, et al. Effector and precursor phenotypes of lymphokine-activated killer cells in mice with severe combined immunodeficiency (scid) and athymic (nude) mice. *Cell Immunol* 1989;120:230–9.
34. Pantelouris EM. Athymic development in the mouse. *Differentiation* 1973;1:437–50.
35. Gershwin ME, Merchant B, Gelfand MC, Vickers J, Steinberg AD, Hansen CT. The natural history and immunopathology of outbred athymic (nude) mice. *Clin Immunol Immunopathol* 1975;4:324–40.
36. Baselga J, Albanell J. Mechanism of action of anti-HER2 monoclonal antibodies. *Ann Oncol* 2001;12 Suppl 1:S35–41.
37. Spiridon CI, Ghetie MA, Uhr J, et al. Targeting multiple Her-2 epitopes with monoclonal antibodies results in improved antigrowth activity of a human breast cancer cell line *in vitro* and *in vivo*. *Clin Cancer Res* 2002;8:1720–30.
38. Romond EH, Perez EA, Bryant J, et al. Trastuzumab plus adjuvant chemotherapy for operable HER2-positive breast cancer. *N Engl J Med* 2005;353:1673–84.
39. Piccart-Gebhart MJ, Procter M, Leyland-Jones B, et al. Trastuzumab after adjuvant chemotherapy in HER2-positive breast cancer. *N Engl J Med* 2005;353:1659–72.
40. Joensuu H, Kellokumpu-Lehtinen PL, Bono P, et al. Adjuvant docetaxel or vinorelbine with or without trastuzumab for breast cancer. *N Engl J Med* 2006;354:809–20.
41. Friedländer E, Arndt-Jovin DJ, Nagy P, Jovin TM, Szöllösi J, Vereb G. Signal transduction of erbB receptors in trastuzumab (Herceptin) sensitive and resistant cell lines: local stimulation using magnetic microspheres as assessed by quantitative digital microscopy. *Cytometry A* 2005;67:161–71.
42. Gennari R, Menard S, Fagnoni F, et al. Pilot study of the mechanism of action of preoperative trastuzumab in patients with primary operable breast tumors overexpressing HER2. *Clin Cancer Res* 2004;10:5650–5.
43. Cartron G, Dacheux L, Salles G, et al. Therapeutic activity of humanized anti-CD20 monoclonal antibody and polymorphism in IgG Fc receptor FcγRIIIa gene. *Blood* 2002;99:754–8.
44. Lazar GA, Dang W, Karki S, et al. Engineered antibody Fc variants with enhanced effector function. *Proc Natl Acad Sci U S A* 2006;103:4005–10.